

The Design and Construction of the Submersible Hybrid Autonomous Rover Craft (SHARC)



Chris Watts*, Jeff Docherty, Alan MacRae, Euan McGookin, Sam Smith, Colin Souza, Jonathan Steen, Jon Trinder, Kerr Vance, Stephen Watson, Kevin Worrall and Daniel Xiaopeng Xi

Faculty of Engineering,
University of Glasgow,
Scotland

www.elec.gla.ac.uk/projects/sharc

ABSTRACT

This paper describes the University of Glasgow's entry into the Defence Science and Technology Laboratories (DSTL) first Student Autonomous Underwater Challenge – Europe (SAUC-E). The objective of this challenge is to design and build an Autonomous Underwater Vehicle (AUV) that can complete a series of underwater tasks. The AUV designed at the University of Glasgow uses an innovative hybrid propulsion system based on a combination of a biomimetic fish tail for forward propulsion and horizontal manoeuvring and conventional propellers for depth control. An overview of the mission strategy is discussed and how the vehicle will accomplish each underwater task. The vehicle, named the Submersible Hybrid Autonomous Rover Craft (SHARC) is equipped with a number of onboard systems including motors, motor drive circuits, Lithium-Polymer battery system, sensors, cameras and a Linux based PC104 single board computer for the main control system. Each of these systems are discussed in some detail along with the design and construction of the various mechanical systems within the SHARC such as the tail propulsion mechanism, custom thrusters and hull.

1. INTRODUCTION

The Student Autonomous Underwater Challenge – Europe (SAUC-E), organised by the Defence Science and Technology Laboratories (DSTL) in association with Heriot-Watt University and the The National Oceanography Centre, is the first event of its kind in Europe. The challenge, based on the 'spirit' of the US AUVSI competition [AUVSI (2006)], is to design and construct an Autonomous Underwater Vehicle (AUV) that can complete a series of underwater tasks in a set time.

Upon hearing of this challenge in November 2005 a team of enthusiastic and dedicated students from the Faculty of Engineering within the University of Glasgow was assembled to design and build an AUV for the Universities entry to the SAUC-E competition.

The SAUC-E challenge comprises four underwater tasks which the vehicle must complete - pass through a validation gate, drop a marker onto a target, touch a mid-water target and surface in a surfacing zone. Points are awarded for the AUV design and performance of the vehicle in the challenge.

This paper will provide a discussion of the vehicle developed for the 2006 SAUC-E challenge at the

* Corresponding Author,
e-mail: c.watts@elec.gla.ac.uk

University of Glasgow. Firstly, the paper gives an overview of the vehicle followed by the strategy that will be employed for the competition tasks. The vehicle is then discussed in some detail giving descriptions of each of the vehicle systems and the rationale behind a number of the design choices.

2. SHARC OVERVIEW

The vehicle developed by the University of Glasgow team is named the Submersible Hybrid Autonomous Rover Craft or SHARC for short. The vehicle, based roughly on the shape and dimensions of a Tiger Shark [Heithaus (2001)], has an innovative 'hybrid' propulsion system based on biomimetic concepts for forward propulsion and manoeuvring and utilizes conventional thrusters for depth control.

The area of Biomimetics (or Bionics or Biomimicry) involves the study and application of methods and concepts found in nature to solve engineering problems [Bar-Cohen (2005)]. In recent years the development of robotic fish and their biomimetic propulsion systems have generated significant interest in the field of Autonomous Underwater Vehicles (AUVs) [McIssac & Ostrowski (2003), Sfakiotakis *et al* (1999)]. This interest is due to the potential benefits of biomimetic propulsion techniques over conventional methods. Benefits such as greater propulsive efficiency can be achieved as shown by MIT in tests with their RoboTuna [Triantafyllou & Triantafyllou (1995)]. MIT's work on their RoboTuna showed that they could achieve higher than 86% efficiency when certain hydrodynamic parameters were within a required range. This compares to efficiencies of around 40% for small propellers used on underwater vehicles.

Another benefit that may be possible with biomimetic propulsion systems is greater agility and manoeuvrability. Certain species of fish can use rapid turning manoeuvres to alter heading by around 180° in less than one body length in a very short period of time [Wolfgang *et al* (1999)]. Due to mechanical limitations of current biomimetic vehicles, this full turning potential may be difficult to realize, however, improvements in manoeuvrability may be possible over conventional underwater vehicles. A study of the turning performance of a robotic fish at Essex University showed that good turning performance was achieved but the turning velocity was still less than that of a real fish [Liu & Hu (2005)]. This was due to the limitations of the mechanics and kinematics of the robot fish in being an approximation to a real fish.

These potential benefits of biomimetic propulsion systems could lead to future AUV's with increased mission duration and with the ability to operate in enclosed environments. These benefits, and the reason for mimicking fish propulsion, stem from the fact that the propulsion technique used by fish has been optimised by millions of years of biological evolution.

It is due to the above reasons that the University of Glasgow vehicle was designed to utilize a biomimetic propulsion system for forward propulsion.

Biomimetic propulsion of the SHARC vehicle is provided by a mechanical tail modelled on the tail propulsion method used by real fish and sharks. Within the area of fish propulsion there are several different methods used by various aquatic species to propel and manoeuvre themselves. The propulsion techniques can be grouped into two broad categories - body and caudal fin (BCF propulsion) and median and paired fins (MPF propulsion) [Colgate & Lynch (2004)]. The majority of fish species use BCF propulsion and it is this method that is used by sharks. This technique for forward propulsion involves passing a propulsive wave along a length of their body. The propulsive wave starts from the anterior of the body and travels towards the caudal fin. It is this undulatory motion that produces a net forward thrust [Videler (1993), Alexander (2003)]. Fish classified as BCF swimmers can be further categorized by how much of their body is used to produce this propulsive wave. Fish that use approximately half of their length to produce the propulsive wave are classified as carangiform [Moyle & Cech (2004)]. As the mechanical shark tail used on the vehicle is approximately half the length of the overall vehicle the SHARC is modelled on this carangiform swimming mode.

Due to the SAUC-E rules concerning buoyancy thrusters are required for controlling the vehicles depth. These thrusters are mounted in the SHARC pectoral fins and were custom made to fit within the fin assembly. A model of the SHARC AUV is shown in Figure 1 below.

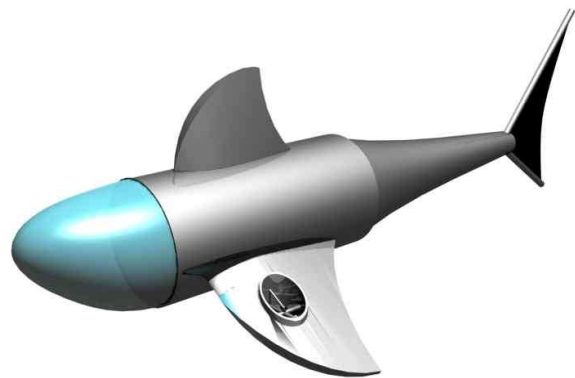


Figure 1: SHARC Vehicle

Overall control of the SHARC is achieved through the implementation of the control algorithm on a Linux based single board computer. Task identification is achieved using a combination of a vision system and sensors.

2.2. SAUC-E Mission Strategy

In order to successfully complete the tasks outlined in the SAUC-E challenge rules [DSTL (2006)] an appropriate mission strategy is required that will factor in the each of the mission objectives, vehicle hardware and the performance of the vehicle. The overall strategy selected is discussed in the following section along with the tactics implemented to complete each individual task.

2.2.1 Overall Strategy

Prior to the start of each competition run the SHARC will be programmed with a set run order in which it will attempt to complete the tasks after successfully navigating the validation gate.

At the start of each allocated competition run an onboard timer will be started that will count the amount of time taken for each task. In order to maximize points, if one task is taking too long then the task will be aborted and the next task undertaken. The amount of time allowed for each task will be proportional to the points available for that task.

2.2.2 Validation Gate

The validation gate is the first task that the AUV must negotiate. The purpose of the validation gate is to show that the vehicle can progress in a controlled manner, in a straight line and at a set depth. Failure to pass through the validation gate will result in the termination of the AUV's current run. Therefore, significant effort has been expended by the team to ensure that the SHARC can successfully pass through the gate.

Two cameras connected to the main control board will be used to detect the upright pipes of the validation gate. Detecting these will allow the SHARC to position itself between the two vertical pipes of the gate and travel through it without touching the sides. The horizontal pipes of the validation gate will be detected using simple sonar transducers.

2.2.3 Mid Water Target

The competition rules state that the mid water target will be an orange object approximately spherical in shape. On detection the SHARC is to travel towards it and touch it.

To do this task a third camera will be set to detect an orange shape. The camera will return the location of the orange area within the current field of view. The camera will be in a front facing position while it is looking for the target. On detection of the target the SHARC will move towards it and contact it with its nose. If the target is not within the current field of view of the SHARC a search pattern will be executed.

2.2.4 Ground Target

The ground target will be located on the floor of the tank. It will consist of a circle, one metre in diameter, with a contrasting cross in the centre and a light beacon located in the middle. The task is to locate this target and drop a marker onto it. The closer the marker is to the target the greater the points awarded.

The approach to this task will be to use the cameras to detect the light from the beacon to locate and home in on the target. For this the central camera will be angled down.

Once the target has been identified and the vehicle will be propelled towards it. As the SHARC passes over the target and the front cameras lose sight of it, the vehicle will glide and the three markers will be dropped using a grapeshot approach (all released at same time).

2.2.5 Surfacing Zone

The surfacing zone is a 3m octagon constructed from PVC pipe located on the surface. An acoustic beacon is located on the bottom of the tank directly beneath the centre of the octagon.

The SHARC will use two acoustic sensors and the vision system to detect and home in on the acoustic beacon. As the SHARC nears the beacon, forward propulsion will cease and full power applied to the vertical thrusters to raise the SHARC to the surface.

3. THE SHARC

The following section gives a brief description of all the mechanical and electrical systems present in the SHARC. Each section discusses briefly the reason behind the methods utilized.

3.1 Power System

Due to the design of the SHARC the power system has to provide power to number of varied electrical systems such as motors and integrated circuits, each with differing power requirements.

The battery system for the SHARC is required to deliver the appropriate current and voltage, continuously for a length of time equal to at least one competition run. As space within the SHARC's main hull is severely limited, the size and weight of any batteries is an issue. Therefore, the power system of the SHARC is based on one 14.8V 12Ah Lithium polymer (referred to as Li-ion's) battery. This battery chemistry was chosen as it offers the best weight/size to energy density ratio of the battery chemistries commercially available today, [Bachmann (2001)]. The current and voltage ratings also exceed what is required.

The power system of the SHARC can be seen in Figure 2.

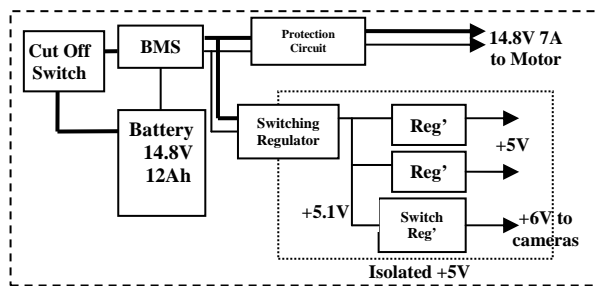


Figure 2: SHARC Power System

The first stage of the power system after the battery is the cut off switch. When the switch is toggled it will cut all power to the SHARC instantaneously. From the cut off switch there is the battery management system (BMS) which is on loan from Reap Systems. The BMS is designed to manage Li-Ion batteries during usage and charging. If any problems with the battery (such as under voltage of a cell or high temperature) occur while the SHARC is operating the BMS will cut the power to the SHARC. This is designed to save the battery and all other SHARC systems and eliminate the risk of any other problems. If the BMS cuts the power while operating a hard reset is required. The BMS will also handle the charging of the battery which will involve the removal of the battery and BMS from the SHARC.

The power to the motors will be supplied, through a protection circuit, directly from the battery. The supply for the lower voltage electronics will be isolated from the motors through an isolated switching regulator. This switching regulator will step the voltage down from 14.8V to 5.1V. A switching regulator was selected due to the efficiency of switching topologies compared to that of linear regulation circuits. To fully achieve the isolation the communication between the electronics and the motor driver circuits will be via opto-couplers.

3.2 Biomimetic Propulsion System

Before design commenced on the biomimetic propulsion system extensive research was undertaken into possible methods for realising the tail motion. The research entailed investigating other biomimetic propulsion systems and robotic fish that have been developed by other academic institutions around the world. From this research the most suitable method appears to be having a central tail spine with a number of segments individually actuated by DC motors. The design methodology behind the selected design was to create a reliable and robust system capable of mimicking the undulatory motion of a shark's tail.

3.2.1 Mechanical Design

At the outset it was decided that the tail was to consist of five independently-powered skeletal segments, based around which would be a flexible exterior shell. Thus, the main decisions to be made were the methods

of powering each segment, connections between segments and material selection. A CAD diagram of the tail segments is shown in Figure 3.

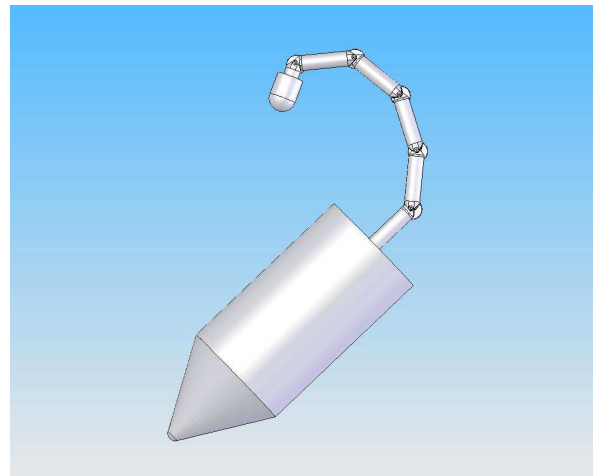


Figure 3: Tail segments

In the interest of keeping the solution simple it was to be constructed, where possible, from readily available materials and components. The design for the tail is based around the single degree-of-freedom manipulation of five separate lengths of rigid plastic piping. Each segment acts as a central spine to which electrical and mechanical components can be attached, as well as structural components for the shape of the tail. The pipe used for the spine segments is 4cm ABS piping, easily available from DIY stores. The only modification to the pipe itself is a 6mm hole drilled at the centre to house a structural aluminium rod.

The joining of the pipe segments is based around compact, interlocking polymer hinges. The bespoke hinges are machined from Nylon66, a material chosen for its self-lubricating properties. To preserve simplicity, the nylon hinge sections are machined to insert into the pipe segments with an interference press fit. The joint transmits torque from the driver segment via a steel shaft pinned to the driven segment. The shaft has flats ground on each end, one for grub-screw connection to a gear and the other for a potentiometer. A diagram of the bespoke hinge used to join each tail segment is shown in Figure 4.

Torque is provided via a 300mNm, 12V DC motor positioned on the underside of each segment (except segment 1 where it is on the top side). A 45° bevel gear is held to the motor output shaft via a brass bush and grub-screw. The gear set-up transmits torque directly to the shaft. The bevel gears are hard wearing acetal copolymer, with a ratio of 1:1 (note, the gears may be changed to similarly dimensioned steel gears after extensive testing).

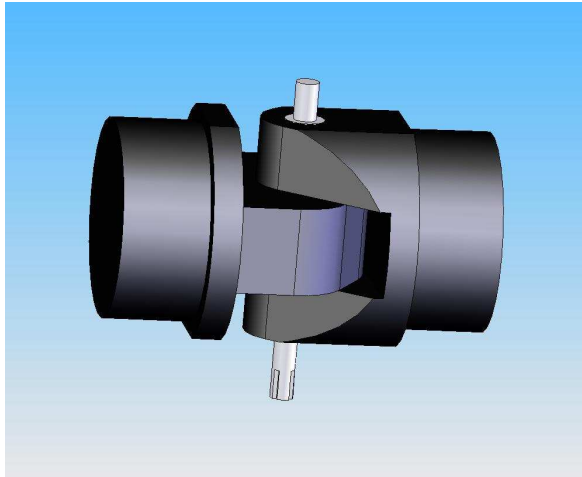


Figure 4: Bespoke tail joint

The motor is held to its relative segment via a two-section housing (see Figure 5 for illustration). The gearbox (125:1) of the motor has three threaded mounting points which are screwed onto a 90° length of angle-section aluminium. The angle-section is mounted on an ABS block shaped to fit the curvature of the pipe. The ABS block is solvent welded to the pipe.

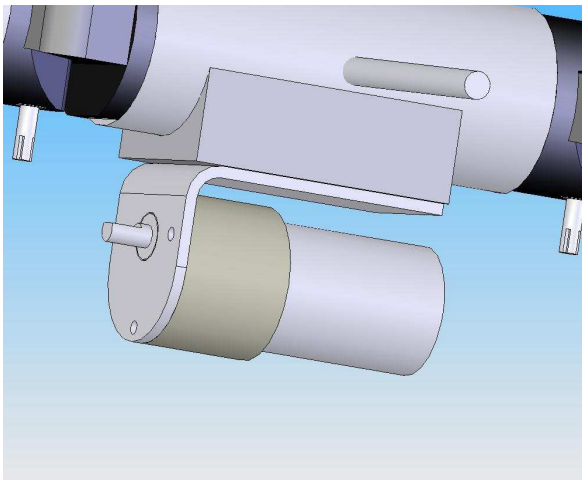


Figure 5: Tail segment motor housing

Segment 1 of the tail is connected to the body section with a large laminated plug as shown in Figure 6. The plug is made from four solvent welded circular sheets of ABS with gussets on the tail side to support the first segment. The pipe segment is extended with a solid section of nylon which runs through the body plug. This allows enough space for the first motor to be mounted on the segment itself, although it must be mounted on the top due to the supporting gusset.

The final segment differs from the first four in that the driven joint section is machined directly from a greater diameter piece of Nylon, forming a bulbous end to which a fin will be attached. Two self-locking

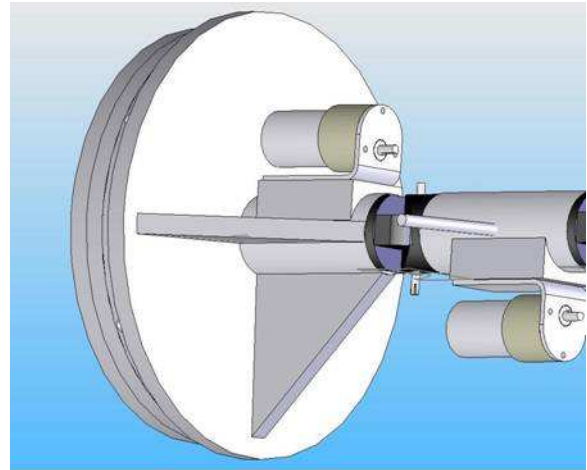


Figure 6: Segment 1 plug

rods are inserted into the bulbous piece and a triangle of flexible rubber sheeting held between them to imitate the caudal fin.

In order for the tail to appear shark like, thin rounded blocks of latex coated Styrofoam are attached to each segment to add bulk to the tail assembly. To provide a flexible waterproof skin for the tail a sleeve manufactured from liquid latex is used.

The completed tail assembly, shown without latex covering and bulking material for clarity, is shown in Figure 7.



Figure 7: Completed tail assembly

3.2.2 Kinematic Based Motor Ratings

In order to specify the motors for each segment of the tail, the tail is regarded as a six degree of freedom robot manipulator [Niku (2001)]. This allows the torque and speed of the motors to be determined through considering the kinematics based *Jacobian*. Firstly, the kinematic relationship between the segments of the tail can be represented using the Denavit-Hartenberg Representation for Forward Kinematics. This representation can be used to determine the speed and torque distribution through the derivation of the associated Jacobian. These are discussed in the following sections.

The Denavit-Hartenberg (DH) representation is based on associating each joint with an appropriately oriented x-z axis. The SHARC tail can be represented by the configuration shown in Figure 8 (i.e. 5 revolute with the fin represented by a static prismatic joint) and the associated joint variables.

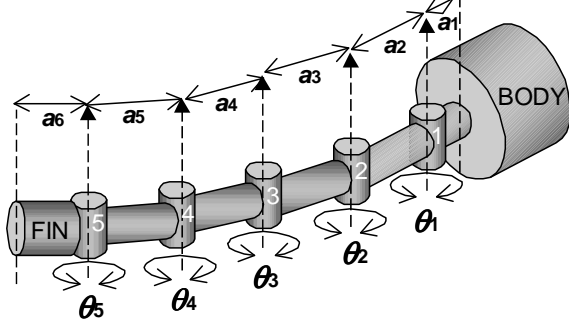


Figure 8: Tail Representation and DH Variables

By considering each joint axes pair and the corresponding variables, the transformation matrices for each joint are defined thus:

$$\mathbf{A}_1 = \begin{bmatrix} C_1 & -S_1 & 0 & a_1 C_1 \\ S_1 & C_1 & 0 & a_1 S_1 \\ 0 & 0 & 1 & 0 \\ 0 & 0 & 0 & 1 \end{bmatrix} \quad (1)$$

$$\mathbf{A}_2 = \begin{bmatrix} C_2 & -S_2 & 0 & a_2 C_2 \\ S_2 & C_2 & 0 & a_2 S_2 \\ 0 & 0 & 1 & 0 \\ 0 & 0 & 0 & 1 \end{bmatrix} \quad (2)$$

$$\mathbf{A}_3 = \begin{bmatrix} C_3 & -S_3 & 0 & a_3 C_3 \\ S_3 & C_3 & 0 & a_3 S_3 \\ 0 & 0 & 1 & 0 \\ 0 & 0 & 0 & 1 \end{bmatrix} \quad (3)$$

$$\mathbf{A}_4 = \begin{bmatrix} C_4 & -S_4 & 0 & a_4 C_4 \\ S_4 & C_4 & 0 & a_4 S_4 \\ 0 & 0 & 1 & 0 \\ 0 & 0 & 0 & 1 \end{bmatrix} \quad (4)$$

$$\mathbf{A}_5 = \begin{bmatrix} C_5 & -S_5 & 0 & a_5 C_5 \\ S_5 & C_5 & 0 & a_5 S_5 \\ 0 & 0 & 1 & 0 \\ 0 & 0 & 0 & 1 \end{bmatrix} \quad (5)$$

$$\mathbf{A}_6 = \begin{bmatrix} 0 & 0 & 1 & 0 \\ 1 & 0 & 0 & a_6 \\ 0 & 1 & 0 & 0 \\ 0 & 0 & 0 & 1 \end{bmatrix} \quad (6)$$

Here the abbreviation S_n stands for $\sin \theta_n$ and abbreviation C_n stands for $\cos \theta_n$. Also, $a_{1..5}$ are the

link lengths between successive joints and a_6 is the length of the caudal fin end segment.

It follows that the total transformation relationship for the fin to the main body of the SHARC is:

$$\begin{aligned} \text{Body } \mathbf{T}_{Fin} &= \mathbf{A}_1 \mathbf{A}_2 \mathbf{A}_3 \mathbf{A}_4 \mathbf{A}_5 \mathbf{A}_6 \\ &= \begin{bmatrix} -S_{12345} & 0 & C_{12345} & \begin{pmatrix} -a_6 S_{12345} + a_5 C_{12345} \\ +a_4 C_{1234} + a_3 C_{123} \\ +a_2 C_{12} + a_1 C_1 \end{pmatrix} \\ C_{12345} & 0 & S_{12345} & \begin{pmatrix} a_6 C_{12345} + a_5 S_{12345} \\ +a_4 S_{1234} + a_3 S_{123} \\ +a_2 S_{12} + a_1 S_1 \end{pmatrix} \\ 0 & 1 & 0 & 0 \\ 0 & 0 & 0 & 1 \end{bmatrix} \quad (7) \end{aligned}$$

The *Jacobian* is a representation of the geometry of the elements of a robot in time. It can be used to convert the differential motions/velocities of individual joints to differential motions/velocities of a particular point of interest. As it defines the individual motions of joints, it can be used to relate these motions to the overall motion of the robot in question. In this case it is used to determine the static forces and torques for the SHARC tail.

It has been found that it is simpler to calculate the Jacobian relative to the last frame, i.e. the *Fin*. Therefore, the force relationship can be written thus:

$$\begin{bmatrix} \text{Fin } \mathbf{f} \end{bmatrix} = \begin{bmatrix} \text{Fin } \mathbf{J} \end{bmatrix} \begin{bmatrix} \boldsymbol{\tau} \end{bmatrix} \quad (8)$$

Here $\text{Fin } \mathbf{f}$ represents the fin's forces and torques in six degrees of freedom, $\boldsymbol{\tau}$ represents the joint forces/torques and $\text{Fin } \mathbf{J}$ is the Jacobian of the fin's reference frame. This expression can be written in the following way:

$$\begin{bmatrix} \text{Fin } f_x \\ \text{Fin } f_y \\ \text{Fin } f_z \\ \text{Fin } m_x \\ \text{Fin } m_y \\ \text{Fin } m_z \end{bmatrix} = \begin{bmatrix} \text{Fin } J_{11} & \text{Fin } J_{12} & \dots & \text{Fin } J_{16} \\ \text{Fin } J_{21} & \text{Fin } J_{22} & \dots & \text{Fin } J_{26} \\ \text{Fin } J_{31} & \text{Fin } J_{32} & \dots & \text{Fin } J_{36} \\ \text{Fin } J_{41} & \text{Fin } J_{42} & \dots & \text{Fin } J_{46} \\ \text{Fin } J_{51} & \text{Fin } J_{52} & \dots & \text{Fin } J_{56} \\ \text{Fin } J_{61} & \text{Fin } J_{62} & \dots & \text{Fin } J_{66} \end{bmatrix} \begin{bmatrix} \tau_1 \\ \tau_2 \\ \tau_3 \\ \tau_4 \\ \tau_5 \\ \tau_6 \end{bmatrix} \quad (9)$$

In order to calculate the force and speed requirements of the joints in the tail, the inverse Jacobian relationship is required. In the case of the force calculation shown in Equation (8), the force vector for the joints, $\boldsymbol{\tau}$, can be determined for a given force and moment configuration for the fin, $\text{Fin } \mathbf{f}$, using the following relationship:

$$\begin{bmatrix} \boldsymbol{\tau} \end{bmatrix} = \begin{bmatrix} \text{Fin } \mathbf{J} \end{bmatrix}^{-1} \begin{bmatrix} \text{Fin } \mathbf{f} \end{bmatrix} \quad (10)$$

However, due to the nature of the Jacobian matrix, its inverse is simply the transposed matrix i.e.

$$[\boldsymbol{\tau}] = [{}^{Fin}\mathbf{J}]^T [{}^{Fin}\mathbf{f}] \quad (11)$$

This relationship is used to determine the torque requirements of the tail's actuators. In order to ensure that the SHARC generated the correct propulsive force, the required force and moments at the Fin are taken to be:

$${}^{Fin}\mathbf{f} = [0.7 \ 0 \ 0.2 \ 0 \ 1.5 \ 0]^T \quad (12)$$

This gives the following torque specifications for each of the tail motors:

$$\boldsymbol{\tau} = [0.5 \ 0.3 \ 0.3 \ 0.2 \ 0.2 \ 0]^T \quad (13)$$

In a similar way to the force distribution calculation in Equation (8), the joint speed distribution can be determined using the application of differential kinematics to the Jacobian. This results in the following relationship:

$$[{}^{Fin}\mathbf{d}] = [{}^{Fin}\mathbf{J}] [d\boldsymbol{\theta}] \quad (14)$$

Here ${}^{Fin}\mathbf{d}$ represents the fin's differential motion in six degrees of freedom and $d\boldsymbol{\theta}$ represents the differential motion of each joint. As with the force calculation, this expression can be written in the following way:

$$\begin{bmatrix} {}^{Fin}dx \\ {}^{Fin}dy \\ {}^{Fin}dz \\ {}^{Fin}\delta x \\ {}^{Fin}\delta y \\ {}^{Fin}\delta z \end{bmatrix} = \begin{bmatrix} {}^{Fin}J_{11} & {}^{Fin}J_{12} & \dots & {}^{Fin}J_{16} \\ {}^{Fin}J_{21} & {}^{Fin}J_{22} & \dots & {}^{Fin}J_{26} \\ {}^{Fin}J_{31} & {}^{Fin}J_{32} & \dots & {}^{Fin}J_{36} \\ {}^{Fin}J_{41} & {}^{Fin}J_{42} & \dots & {}^{Fin}J_{46} \\ {}^{Fin}J_{51} & {}^{Fin}J_{52} & \dots & {}^{Fin}J_{56} \\ {}^{Fin}J_{61} & {}^{Fin}J_{62} & \dots & {}^{Fin}J_{66} \end{bmatrix} \begin{bmatrix} d\theta_1 \\ d\theta_2 \\ d\theta_3 \\ d\theta_4 \\ d\theta_5 \\ d\theta_6 \end{bmatrix} \quad (15)$$

This allows small motions in the fin to be calculated for the associated small motions in each of the joints.

Similarly the speed calculation for the joints is achieved using the Jacobian's transpose:

$$[d\boldsymbol{\theta}] = [{}^{Fin}\mathbf{J}]^T [{}^{Fin}\mathbf{d}] \quad (16)$$

For this application the required speeds at the Fin are taken to be:

$${}^{Fin}\mathbf{d} = [4.0 \ 0.0 \ 1.0 \ 0.0 \ 100.0 \ 0.0]^T \quad (17)$$

It should be noted that the first 3 elements are in m/s and the last 3 are in rpm. This gives the following speed specifications, in rpm, for each of the tail motors:

$$d\boldsymbol{\theta} = [20 \ 20 \ 20 \ 20 \ 20 \ 0]^T \quad (18)$$

The combination of the torque and speed ratings for Equations (13) and (18) provided the specifications for the motors used the biomimetic tail propulsions system. The operational specifications for the actual motors used are given in Table 1.

Table 1: Motor Specifications

Joint	Motor	Torque	Speed
1	Crouzet 12V Geared 3.9W	0.5Nm	45rpm
2	Trident IG33, 12V Geared	0.3Nm	29rpm
3	Trident IG33, 12V Geared	0.3Nm	29rpm
4	Trident IG33, 12V Geared	0.3Nm	29rpm
5	Trident IG33, 12V Geared	0.3Nm	29rpm

3.2.3 Tail Electronics & Motor Control

The biomimetic tail propulsion system has two levels of control, firstly the control of the motion of each segment and then the control of the overall tail motion. Control of each of the five tail segments is achieved using a motor feedback potentiometer, a PIC16F88 microcontroller and an L6202 motor drive circuit. During operation each segment receives an instruction from the main tail controller via a Controller Area Network (CAN) bus containing the angle that particular segment should be at that time. The PIC16F88 translates this desired angle into a voltage and utilizes a proportional control algorithm to move the motor accordingly until the desired voltage is obtained from the motor feedback potentiometer. The speed at which messages are sent from the main tail controller determines the overall speed of the tail movements.

Overall control of the tail movement is the responsibility of the tail controller. This controller receives desired heading and speed information from the higher level Guidance and Navigation Control System (GNCS) and translates it into a sequence of movements of each tail segment. The sequence of movements is communicated to each segment via the CAN bus.

3.3 Main Body/Hull

The SHARC body is comprised of two hulls, an inner and outer hull. The outer hull is constructed from 22cm diameter, 0.8cm thick, PVC pipe. Attached to this hull are two pectoral and one dorsal fin, the lifting points, a belly section and the mechanical tail plug.

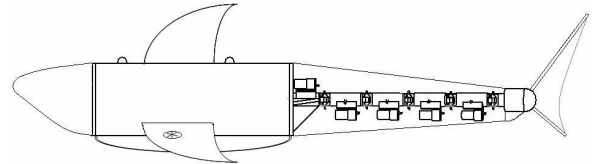


Figure 9: SHARC Diagram

The inner hull is also manufactured from PVC pipe of slightly smaller diameter than the pipe used for the outer hull. A removable waterproof bulkhead is attached onto the rear of the inner hull. All electrical through hull connections are made using suitable

waterproof connectors and as an additional precaution a latex seal is used wherever possible. Within the inner hull there is a removable tray on which the electronic control boards and batteries are located to allow for easy removal.

3.3.1 Head section

The head section is manufactured from transparent Perspex. This will allow cameras to be mounted within the head and have a clear field of vision. In order to reduce distortion, the locations within the Perspex where the cameras view through are designed to be flat. The shape of the head is a compromise between the shape required by the cameras and the shape of a real tiger shark. Fabrication of the Perspex head was achieved using a vacuum forming process and a carved wooden mould.

3.3.2 Marker Design & Release System

In order to complete the task which requires a marker to be dropped onto a target a suitable marker and marker release system is required. It was decided that to limit the number of through hull connections that a magnetic release system should be used. This method requires that the marker is magnetic and is held onto the underside of the hull by another powerful magnet which can be moved. To move the magnet within the hull a magnet will be attached to a spring compact return solenoid. Once the magnet within the hull has been moved away from the marker the force holding the marker to the hull will be reduced and so the marker will fall.

The markers to be released by the SHARC are constructed from a 3.5cm model submarine brass propeller, an egg cup, a small bag of lead shot and a magnet to attach it to the hull. A diagram of the marker is shown in Figure 10. Once released the propeller should ensure the marker has a smooth trajectory to the tank floor. On impact the bag of lead shot should deform to absorb the impact and so stop the marker from moving or rolling.

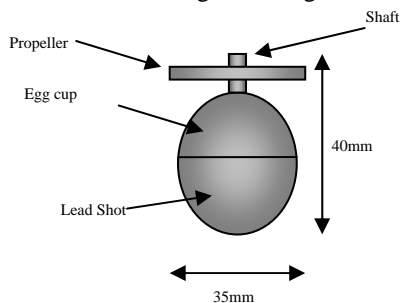


Figure 10: Marker design

3.4 Fins

The SHARC design specifies three stabilising fins, composed of two pectoral fins which are inclined downwards at an angle of 30° to the horizontal, and

one vertically-mounted dorsal fin. This configuration was selected as it is in keeping with the appearance of a Tiger shark, on which the SHARC is based.

SAUC-E rules require that entries be negatively buoyant, and so the purpose of the pectoral fins is to generate a downwards force as the vehicle travels through the water. Thrusters are also mounted in these fins in order to control pitch and so moderate the surface/dive rate of the vehicle. The purpose of the dorsal fin (which is also fixed) is to provide roll stability control.

3.4.1 Design

When considering the profiles of control surfaces, particular attention must be paid to the important aerodynamic ratio that is the Reynolds Number. This is defined as the ratio of inertial forces to viscous forces within the fluid flow. When cruising, the SHARC will be in the Reynolds Number region of around 4.5×10^5 . The NACA 0015 aerofoil is particularly suitable for use in this low Reynold's number region [Galbraith & Coton (2006)]. The cambered NACA 4415 is also gives good performance, [Galbraith & Coton (2006)], however, the camber makes this more difficult to fabricate, and so the NACA 0015 (see Figure 11 below) was selected for all three fins for the SHARC.

The thrusters were to be fitted at the thickest part of the fin. On the NACA 0015, this is at approximately $1/3$ of the chord measured from the leading edge.

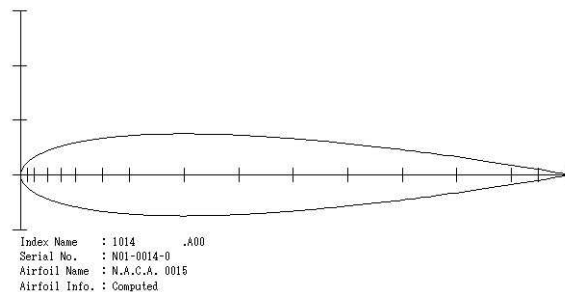


Figure 11: NACA 0015 Aerofoil

In order to generate downforce, the selected NACA 0015 fins had to be set at a small negative angle to the oncoming (freestream) flow. Clearly, the faster the vehicle velocity the greater the force that is produced for a given inclination. Bernoulli's force equation was used to estimate the amount of downforce generated at various angles of incidence. At this stage, the cruising speed of the SHARC was assumed to be 1.5 ms^{-1}

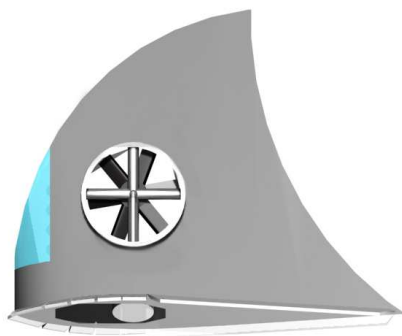
The simple analysis carried out provided estimates rather than exact force values. The thruster fixed in each fin will modify the flow over this portion of the control surface, and allowances must be made for a reduction in the forces produced due to tapering from root to tip, and from tip vortex effects.

In nature these fins are flexible, controlled by muscles to provide a fluid motion in order to accurately control the movement of the creature. As it would be too complicated to build fins with these exact characteristics in the first revision of the SHARC their function had to be replicated as closely as possible. For simplicity it was decided that the pectoral fins would be rigid, with the small vertical thrusters to control roll and to provide depth control. The dorsal fin would simply be a rigid fin with correct hydrodynamic properties to maximize stability.

The leading edge of all three fins must have a rough finish, in order to promote transition to turbulent flow, as laminar fluid flow is prone to flow separation at these low Reynolds Numbers. Flow separation would result in a substantial increase in drag and the performance of the vehicle would be compromised. Roughness is also applied at the join of the main body section with the head piece.

3.4.2 Construction

The fins are mounted onto the main body at approximately 30° and the thruster crevice is angled appropriately to give direct vertical thrust. The fins also feature a high-power LED array housed inside a small Perspex case along the front edge for low-visibility situations. The whole fin is attached to the main body by an aluminium flange that runs around the edge of the fin. The flange has holes where bolts can be located to attach the fin to the outer hull. The inside of the fin, where the motor assembly is housed, can then be accessed in case of problems. A rubber edge around the fin will ensure a water tight seal.



Pictorial Fin plan elevation

Figure 12: CAD Drawing of complete fin

To increase buoyancy the fins are made from high density blue Styrofoam. The main fin forms were cut using hot wires and sanded down to give a smooth shape. The thruster and the LED slot were cut and the thruster assembly was inserted and glued in place. The aluminium flange was then produced and glued into place. To increase the strength of the fins and to prepare them for the strengthening fiberglass, the fins are coated with U-POL, a polyfiller type product. The inside of the fins can be partially hollowed out at this

point for the motor and the LED array and inserted and glued into place. A Perspex window was also constructed to cover the LED array and also glued in place. A rubber edge is cut and glued around the edge of the fin to ensure a watertight connection. The entire fin was then coated with fiberglass to maximize strength and finally coated with Latex to ensure a proper watertight seal and to match the rest of the craft. A similar process is repeated for the dorsal fin but with no thruster assembly. All three fins are attached to the outer hull using bolts.

3.4.3 Thruster Assembly

Due to the size and shape of the pectoral fins on the SHARC vehicle it was difficult to source appropriate 'off the shelf' thrusters that could be used for depth control. Therefore, custom thrusters have been designed and constructed which fit into the space available in the pectoral fins. Six blade 7cm diameter model submarine propellers mounted vertically in the fins are connected via a universal joint and a stern tube to a high speed DC motor housed within the fin. The shaft is supported by two aluminium rods that hold a small bearing in the centre. This assembly is housed inside a PVC tube and glued into the thruster crevice. The DC motor and drive circuitry has been waterproofed as an added precaution.

3.5 Sensors

To allow the SHARC to successfully complete the challenge a number of sensors are required.

For basic obstacle avoidance and ranging a series of ultrasonic sonar transducers are positioned around the hull. Simple 40 kHz waterproof transducers are used to produce bursts of sound which will reflect off solid object underwater. As the speed of sound in water is known the time between transmission and reception of the reflected signal will allow the range of an object to be determined (see Figure 13 for illustration). The SHARC AUV has five banks of these ultrasonic rangars, one facing directly forward and four positioned around the head angled slightly off centre.

The ultrasonic rangars are used for to detect nearby objects for obstacle avoidance purposes. They will also allow for detection of the upper and lower horizontal bars of the validation gate.

A pressure sensor is utilized to determine the current depth of the vehicle. The sensor, positioned in the belly of the SHARC, produces depth measurements which are passed to the main control system via the CAN bus.

The SHARC will also be fitted with a solid state accelerometer and rate gyroscope. These will allow the forward velocity and yaw of the vehicle to be measured. These parameters will be fed to the main control system and along with the vision system are vital elements for the control strategy implemented.

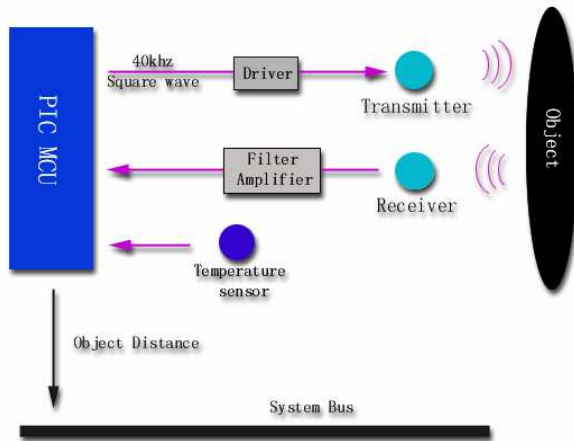


Figure 13: Ultrasonic obstacle avoidance

3.6 Head & Vision System

The aim of the vision system is to successfully identify the underwater targets and provide part of the necessary navigation information to the control algorithms within the main control system.

The vehicle is equipped with one USB and two CMUcam2+ cameras. By utilising the CMUcam2+ we can take advantage of the on board image processing abilities and reduce the processing strain on the embedded Linux single board computer. The captured and processed images will provide heading information relating the vehicle's present heading (vehicle based frame of reference) to the acquired target i.e. the validation gate. In order to relate this heading angle to an Earth based frame of reference the information will have to be combined with data from the on board rate gyros.

The cameras will be housed at the front of the vehicle contained within a perspex head and arranged in the configuration shown in Figure 14.

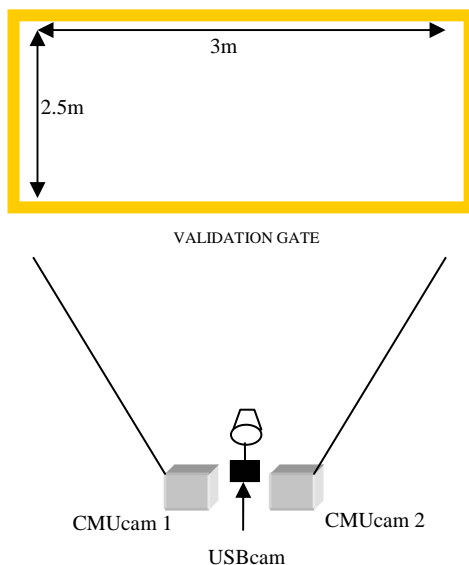


Figure 14: Positioning of cameras

The CMUcams are positioned such that they detect the uprights of the validation gate. This method is necessary due to the dimensions of the validation gate and the field of view of the single camera. The distance to the validation gate can also be obtained as the dimensions of the gate are known; the apparent size of the target can be related to the distance from the object. The CMUcam will be able to determine the centre coordinates of the detected uprights by searching for orange 'blobs'. The cameras can be aligned so that the images 'meet' and a larger field of view can be created, as demonstrated by Figure 15. The breadth of the target (in pixels) is calculated and related to the 3m's, creating a photo scale. This then allows for the distance D1 to be calculated. Using the distances D1 and D2 and utilising simple trigonometry the heading angle to the target can be found.

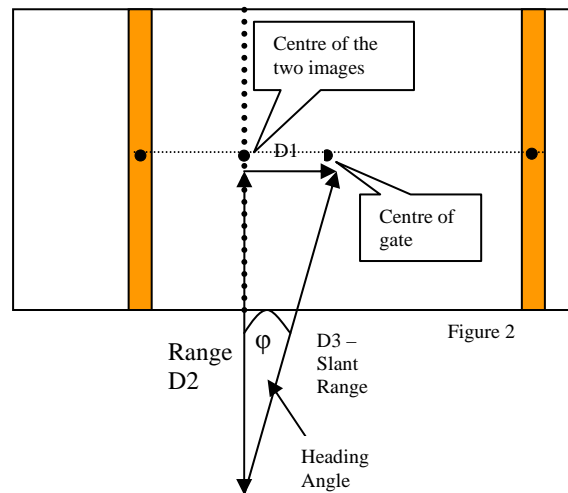


Figure 15: Combination of camera views

The image processing algorithms will be developed within a C programming environment. Preliminary research and development was carried out using MATLAB. However due to restrictions on the portability of MATLAB standalone applications within an embedded system this possibility was rejected.

The USB camera will use servos to position the camera $\pm 90^\circ$ from the forward looking position. This system will be used to locate the contrasting cross situated at the bottom of the tank. Using the USB camera provides a higher resolution image and a greater likelihood of detecting the target. The CMUcams both draw 200mA's each. When not in use the cameras will be put into a 'sleep mode' to save power.

The surfacing gate will be detected by positioning the USB cam to the $+90^\circ$ position. Information relating to the octagonal target will be derived from the webcam image while being fused with information from the acoustic beacon associated with the target.

3.7 Guidance and Navigation Control System

The GNCS controls the manoeuvring capability of the SHARC. The control of the motion in heading and depth, as well as regulating the speed of the vehicle, is achieved through 3 single input, single output (SISO) control loops, as shown in Figure 16.

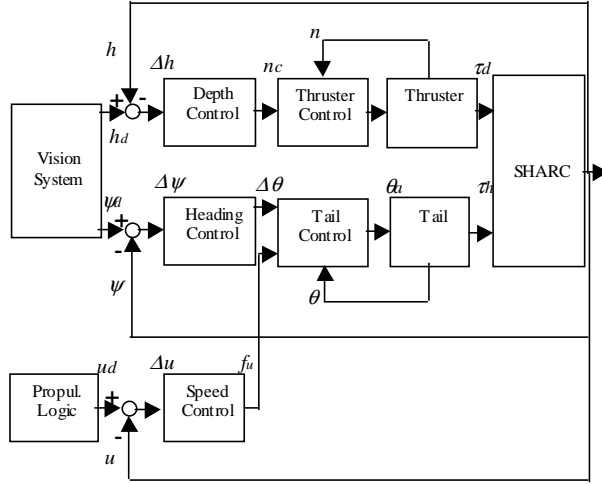


Figure 16: Guidance and Navigation Control System Diagram

The three loops control the heading and speed through the force produced by the tail (τ_h) and the depth through the resultant thrusters' force (τ_d). Each of these is discussed in the following sections.

3.7.1 Propulsion Control

The propulsion or speed control system determines the beat frequency of the SHARC's tail [Alexander (2003)]. It follows that if the frequency is high then the undulation of the tail will be fast. This results in a greater propulsive force. For constant forward motion in surge the tail will displace an equal amount of water on each side of its body (see Figure 17 for an illustration). This balanced deflection ensures constant forward motion.

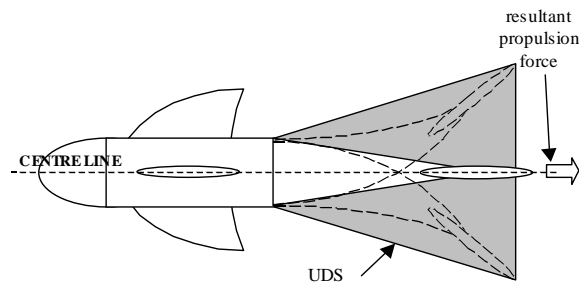


Figure 17: Forward Motion Using Undulation

The resulting undulation creates a wedge of movement around the tail. This wedge is referred to the

Undulation Displacement Segment (UDS). For forward motion the area of the UDS on each side of the central line of the SHARC is the same.

In order to ensure that the SHARC is moving at the desired forward or *surge* speed (u_d), the actual speed of the vehicle (u) is measured and compared with the desired propulsion rate. This produces an error signal ($\Delta u = u_d - u$) which is used by the speed controller to drive the actual speed towards the desired speed and thus minimise the error. The speed controller generates a commanded beat frequency for the tail (f_u) and the structure of the controller is based on a simple PID controller [Franklin *et al* (1991), Dutton *et al* (1997)]:

$$f_u = K_{pp} \Delta u + K_{ip} \int \Delta u dt + K_{dp} \frac{d\Delta u}{dt} \quad (19)$$

With suitable values chosen for the controller gains, this control scheme is able to control the frequency of undulation of the tail and thus regulate the surge velocity of the vehicle. The frequency of undulation is used by the tail controller to determine the motion of each motor in the tail.

3.7.2 Heading Control

The heading control system regulates the manoeuvring capability of the SHARC by manipulating the deflection of the tail while it is undulating. As discussed in Section 3.7.1, the undulating tail produces an UDS that generates the propulsive thrust for the vehicle. If this UDS is deflected away from the centre line of the vehicle, then the forces on each side of the SHARC are unbalanced. This results in a turning moment that can be used to manoeuvre the vehicle and thus change its heading. The amount that the UDS is deflected from the balanced centre line determines the amount of turning that the tail can generate. Port and Starboard manoeuvres are illustrated in Figure 18, showing the effect of the UDS deflection on the yawing moment of the SHARC.

In this case $\Delta\theta$ is the deflection of the UDS and it is generated by the heading controller as shown in Figure 16. The heading controller produces this deflection based on the comparison of the desired heading angle (ψ_d) and the actual heading of the vehicle (ψ). The comparison generates the heading error ($\Delta\psi = \psi_d - \psi$) which is used in the heading controller calculation as shown in Equation (20) below.

$$\Delta\theta = K_p \Delta\psi + K_i \int \Delta\psi dt + K_d \frac{d\Delta\psi}{dt} \quad (20)$$

With the selection of appropriate gains for this PID structure, the controller generates a deflection command that minimises the heading error and thus drives the actual heading toward the desired heading. This provides the necessary manoeuvring capability to the SHARC.

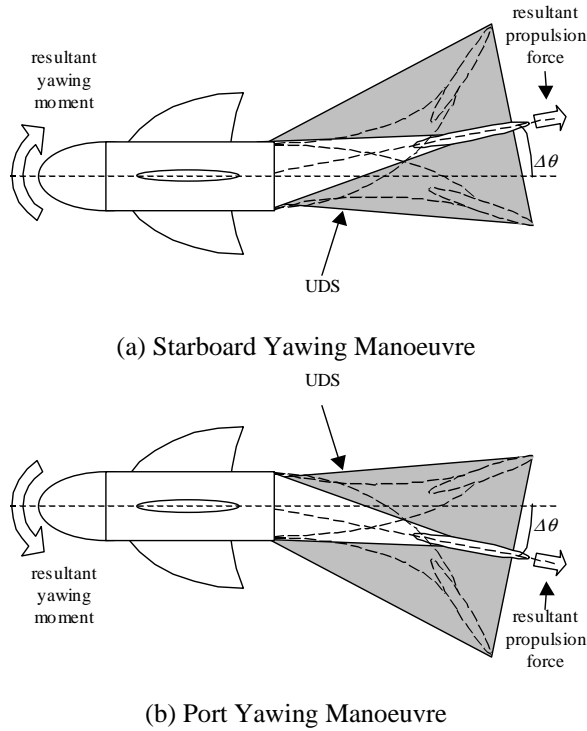


Figure 18: UDS Deflection for Yawing Manoeuvres

3.7.3 Depth Control

The depth control loop regulates the force produced by the pectoral fin thrusters. The combination of both thrusters allows the SHARC to govern what depth it is operating at. The reference for the desired depth (h_d) comes from the fusion of data from the vision system and the ultrasonic sensors. This desired operating depth is compared with the actual depth of the vehicle (h) to produce a depth error measurement ($\Delta h = h_d - h$). The depth control uses this error to drive the actual depth of the vehicle towards the desired operational depth. The resultant controller is based on a simple PID structure and produces the commanded thrusters speed, n_c [Fossen (1994), Franklin *et al* (1991), Dutton *et al* (1997)]:

$$n_c = K_{pd}\Delta h + K_{id} \int \Delta h dt + K_{dd} \frac{d\Delta h}{dt} \quad (21)$$

With suitable values chosen for the controller gains, this control scheme is able to control the speed of rotation of the thrusters. This command is sent to an inner-loop regulator that ensures that the actual speed of the thrusters follows the commanded speed generated from Equation (21). This combined with the Propulsion and Heading Controllers enables the SHARC to manoeuvre effectively within the underwater environment.

3.7.4 GNCS Implementation

The SHARC GNCS is implemented on a Linux based PC104 single board computer very generously donated by Arcom.

4. CONCLUSIONS

The SHARC vehicle has been designed to be a functional craft constructed from low cost, readily available materials that proves the viability of biomimetic propulsion systems for AUV's. Whilst being constructed primarily for the first DSTL SAUC-E competition, the modular design of the mechanical and electronic systems within the craft allow for easy upgrades and modifications. It is intended to be a platform which can be used to investigate and optimize all aspects of fish-tail biomimetic AUV's including propulsion, navigation and guidance and control. Imitation of a shark at a length of around 1.75m provides sufficient capacity for a larger payload than most robotic fish prototypes developed to date. This increases the versatility and adaptability of the SHARC.

Overall, the development of the SHARC has provided the team at the University of Glasgow with the experience and a knowledge-base that gives a solid foundation for future work on AUV's, both biomimetic and conventional, which can also be applied to participation in future SAUC-E challenges.

ACKNOWLEDGEMENTS

The University of Glasgow AUV Team would like to take this opportunity to thank all of the companies and organizations that sponsors and supports our team:

University of Glasgow Organizations-

Dept of Aerospace Engineering, Dept of Electronics & Electrical Engineering, Dept of Mechanical Engineering, Dept of Civil Engineering and the Faculty of Engineering.

Industrial Sponsors-

Arcom www.arcom.com
 Analog Devices www.analog.com
 Reap Systems Ltd. www.reapsystems.com
 EPSRC www.epsrc.ac.uk

The University of Glasgow AUV Team would also like to thank the following people for their assistance and support with this project: Ian Brown and Tony Smedley, Dept of Aerospace Engineering, for all the time, effort and advice they gave to the team, Stuart Mclean, Dept of Civil Engineering, University of Glasgow for his encouragement and allowing the team to use the Civil Engineering Water Laboratories, Shona Ballantyne and Stuart Fairbairn, Dept of Electronics & Electrical Engineering, for all their assistance in ordering the many unusual parts and components the team required, Dr D. Muir, Dept of Electronics & Electrical Engineering, for his support and allowing the team access to electronics laboratory space.

REFERENCES

- AUVSI, (2006), *AUVSI and ONR's 9th International Autonomous Underwater Vehicle Competition*, The Association for Unmanned Vehicle Systems International, <http://www.auvsi.org/competitions/water.cfm>, May 2006
- Alexander, R.M., (2003) *Principles of Animal Locomotion*, Princeton University Press.
- Bachmann, I., (2001), *Batteries in a Portable World: a handbook on rechargeable batteries for non-engineers*, Cadex Electronics Inc.
- Bar-Cohen, Y., (2005), "Biomimetics: mimicking and inspired-by biology", Jet Propulsion Lab, California Institute of Technology, *Proceedings of the SPIE Smart Structures Conference*, San Diego, CA., SPIE Vol. 5759-02
- Colgate, J.E. & Lynch, K.M., (2004), "Mechanics and Control of Swimming: A review", *IEEE Journal of Oceanic Engineering*, Vol 29, No 3.
- DSTL, (2006), DSTL Official Website, SAUC-E rules, http://www.dstl.gov.uk/news_events/competitions/sauc/mission-rules-06.pdf, May 2006
- Dutton, K., Thompson, S. & Barraclough, B., (1997) *The Art of Control Engineering*, Addison-Wesley, Harlow
- Fossen, T.I., (1994) *Guidance and control of ocean vehicles*. John Wiley and Sons Ltd., Chichester.
- Frankin, G.F., Powell, J.D. and Emami-Naeini, A., (1991), *Feedback Control of Dynamic Systems*, 2nd Edition, Addison Wesley
- Galbraith, R. & F.N. Coton., (2006) "A review of low reynolds number aerodynamic research at the University of Glasgow", R.A.MCD. Department of Aerospace Engineering, University of Glasgow.
- Heithaus, M. R., (2001), "The biology of tiger sharks, *Galeocerdo cuvier*, in Shark Bay, Western sex ratio, size distribution, diet, and seasonal changes in catch rates", *Environmental Biology of Fishes* **61**: 25–36, 2001.
- Liu, J. & Hu, H., (2005), "Mimicry of Sharp Turing Behaviours in a Robotic Fish", *Proceedings of the IEEE International Conference on Robotics and Automation*, pp3329-3334
- McIssac, K.A. & Ostrowski, J.P., (2003), "Motion Planning for Angulliform Locomotion", *IEEE Transactions on Robotics and Automation*, Vol 19, No 4
- Moyle, P.B. & Cech, Jr, J.J., (2004), *Fishes: An Introduction to Ichthyology*, 5th Edition, Prentice Hall, Inc.
- Niku, S.B., (2001), *Introduction to Robotics: Analysis, Systems, Applications*, Prentice Hall
- Sfakiotakis, M., Lane, D.M. & Davies, B.C. (1999) Review of Fish Swimming for Aquatic Locomotion, *IEEE Journal of Oceanic Engineering*, Vol. 24, No. 2, pp 237-252.
- Triantafyllou, M.S. & Triantafyllou, G.S., (1995), "An Efficient Swimming Machine", *Scientific America*
- Tzeranis, D., Papadopoulos, E. & Triantafyllou, G.S. (2003) On the Design of an Autonomous Robot Fish, *Proceedings of 11th IEE Mediterranean Conference on Control and Automation*, Rhodes.
- Videler, J.J., (1993), "Fish Swimming", *Fish and Fisheries Series 10*, Chapman & Hall
- Wolfgang, M.J., Anderson, J.M., Grosenbaugh, M.A., Yue, D.K.P., Triantafyllou, M.S., (1999), "Near-body Flow Dynamics in Swimming Fish", *The Journal of Experimental Biology* 202, p 2303-2327